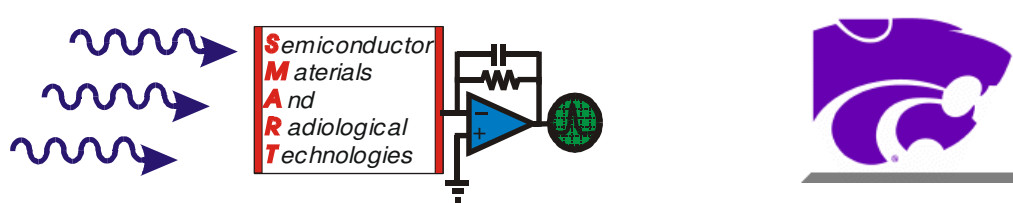


# Semiconductor Radiation Detectors with Frisch Collars and Collimators for Gamma Ray Spectroscopy and Imaging

(DOE NEER Grant Number 03ID14498)

Douglas S. McGregor, Alireza Kargar, Mark Harrison, Adam Brooks,  
Walter McNeil, Rans B. Lowell and Adam Graebner

Semiconductor Materials and Radiological Technologies Laboratory  
Department of Nuclear and Mechanical Engineering  
Kansas State University  
Manhattan, KS 66506



Submitted to the

Department of Energy

Nuclear Engineering and Educational Research Program

December 2006

NFAA DE-FG07-031D14498

Technical Progress Report for year 3 covering the period  
July, 2003 – Present

## **Semiconductor Radiation Detectors with Frisch Collars and Collimators for Gamma Ray Spectroscopy and Imaging**

Douglas S. McGregor, Alireza Kargar, Mark Harrison, Adam Brooks, Walter McNeil,  
Rans B. Lowell and Adam Graebner  
SMART Laboratory, Kansas State University, Manhattan, KS 66506

**Project Title:** Semiconductor Radiation Detectors with Frisch Collars and Collimators for Gamma Ray Spectroscopy and Imaging

**Covering Period:** July 2003 - present

**Date of Second Report:** Dec. 4, 2006

**Recipient:** Kansas State University  
2 Fairchild Hall  
Manhattan, KS 66506

**Award Number:** DE-FG07-031D14498

**Subcontractors:** None

**Other Partners:** None

**Contact:** Douglas McGregor  
(785) 532-5284  
mcgregor@ksu.edu

**Project Team:** Nancy Elizondo

**Project Objective:** To study CdZnTe as a high energy resolution gamma ray detector with a novel new design, and to build a detector array from the new detector design.

**Status:**

**CdZnTe Growth** It was learned that commercial companies refused to sell CdZnTe material to Kansas State University out of fear that the technologies being developed at KSU were competitive to their products, mainly eV Products and YinnelTech. As a result, KSU was forced to grown

their own material for this work. The KSU custom multizone vertical Bridgman furnace has been put into operation for CdZnTe crystal growth. Quartz ampoules are used to grow CdZnTe. Typically a vitrified carbon coating is adhered onto the inside of the quartz ampoules before vertical Bridgman growth. A well-defined and repeatable process to carbon coat and vitrify the adhered carbon has been developed. A paper on the process has been published. Several CdZnTe ingots have been grown.

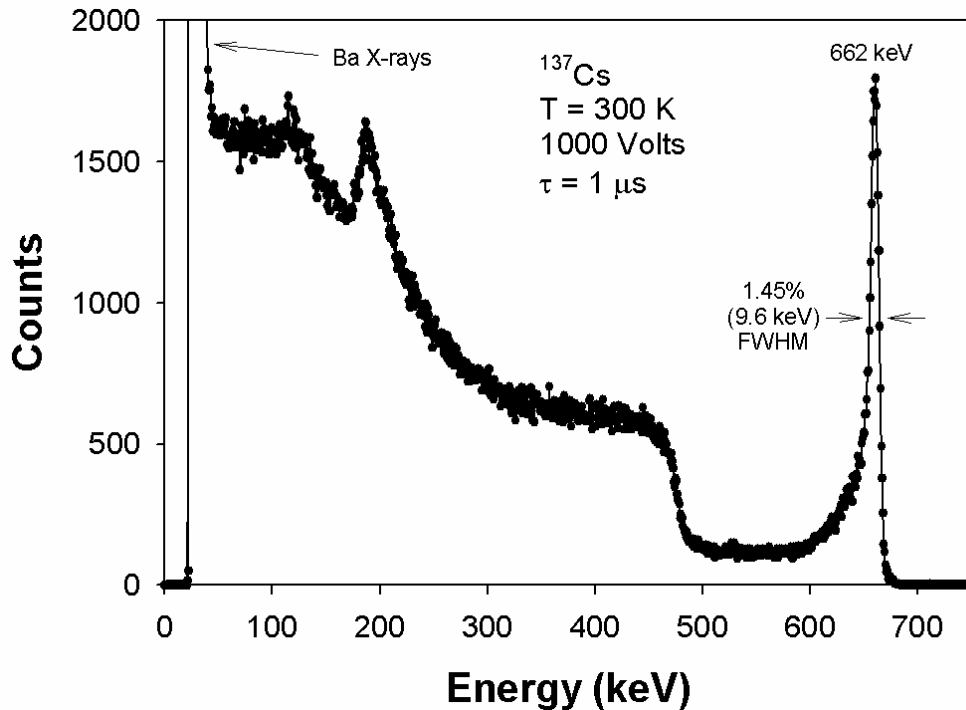
**CdZnTe Detector  
Fabrication**

A process has been developed to mass-produce CdZnTe bar-shaped pieces for Frisch ring detectors. Researchers at Brookhaven National Laboratory have assisted with the process, and have taken a special interest in this particular NEER project. The devices are cut and polished with precision lapping tools. Contacts are applied with electroless gold, and the sides are passivated with a hydrogen peroxide solution. The devices are then wrapped in Teflon tape and inserted into copper Frisch rings. World record results have been realized over the past year.

**CdZnTe Detector  
Testing**

A special laser aligned characterization platform has been designed and built to study the directionality of the collimated Frisch ring detectors. Numerous collimators, formed from extruded tungsten, have been purchased to assemble the Frisch ring array. Tests thus far clearly indicate that the devices, after insertion into the collimators, have a salient sensitivity in the forward direction. Further, devices have been demonstrated for samples ranging in size from 3 x 3 x 6 mm up to 6 x 6 x 12 mm. All sizes have demonstrated incredible energy resolution for  $^{137}\text{Cs}$ , being approximately 1.5% FWHM. Some devices have demonstrated energy resolution of 1.15% FWHM or less. The device design won an R&D 100 award

for year 2005, and two patents have been allowed on the design, those being: US-6,175,120 and US-6,781,132.



Energy spectrum from a 3 x 3 x 6 mm CdZnTe Frisch ring bar detector, showing energy resolution of 1.45% FWHM.

**Future plans:** CdZnTe ingots will be grown using high-quality ultra-pure (6 nines) Cd, Zn, and Te materials. The ingots will be characterized and Frisch Collar radiation detectors will be fabricated from the material. A set of 32 Frisch Collar high-resolution semiconductor gamma ray spectrometers will be completed into an array, using two separate 16-element modules. The micro-electronics needed to operate the modules will be completed and attached to the modules. These powerful devices can be commercialized for a variety of other applications for radiation dosimetry and homeland security.

**Publications resulting from this work:** 1. M.J. Harrison, A. Kargar, D.S. McGregor, "Charge Collection Characteristics of Frisch Collar CdZnTe Gamma Ray Spectrometers," Nucl. Instrum. And Meth. A, (2006) in review.

**cont.**

2. A. Kargar, A.M. Jones, W.J. McNeil, M.J. Harrison, and D.S. McGregor, "Angular Response of a W-Collimated Room-Temperature-Operated CdZnTe Frisch Collar Spectrometer," Nuclear Instrum. and Meth., A562 (2006) pp. 262-271.
3. A.E. Bolotnikov, G.S. Camarda, G.A. Carini, M. Fiederle, D.S. McGregor, W. McNeil, G.W. Wright, and R. B. James, "Performance Characteristics of Frisch-Grid CdZnTe Detectors," IEEE Trans. Nuclear Science, vol. NS-53 (2006) pp. 607-614.
4. M. J. Harrison, A.P. Graebner, W.J. McNeil, and D.S. McGregor, "Carbon-Coating of Fused Silica Ampoules," Journal of Crystal Growth, 290 (2006) pp. 597-601.
5. A. Kargar, A.M. Jones, W.J. McNeil and D.S. McGregor, "CdZnTe Frisch Ring Detectors for Gamma Ray Spectroscopy," Nuclear Instrum. and Meth., A558 (2006) pp. 497-503.
6. A.E. Bolotnikov, G. S. Camarda, G. A. Carini, G. W. Wright, R. B. James, D. S. McGregor, and W. McNeil, "New Results from Performance Studies of Frisch-Grid CdZnTe Detectors," Proc. SPIE, Vol. 5540 (2004) pp. 33-45.
7. W. J. McNeil, D. S. McGregor, A. E. Bolotnikov, G. W. Wright, R.B. James, "Single Charge Carrier Type Sensing with an Insulated Frisch Ring CdZnTe Semiconductor Radiation Detector," Applied Physics Letters, 84 (2004) pp. 1988-1990.

**Conference  
Proceedings**

1. D.S McGregor, A. Kargar, W.J. McNeil, M.F. Ohmes, B. Rice, J.K. Shultis, T. Unruh, "Detector Development in the Kansas State University SMART Laboratory," ANS Topical Meeting, Albuquerque, NM, Nov. 12-16, 2006..
2. Y. Cui, Member, A. E. Bolotnikov, G. S. Camarda, G. De Geronimo, P. O'Connor, R. B. James, A. Kargar, M. J. Harrison, and D. S. McGregor, "Readout System for Arrays of Frisch-ring CdZnTe

- cont.** Detectors,” IEEE Nuclear Science Symposium, San Diego, CA, Oct. 29-Nov. 3, 2006.
3. K. C. Mandal, S. H. Kang<sup>1</sup>, M. Choi, D. Rauh, A. Kargar, M. J. Harrison, D. S. McGregor, A. E. Bolotnikov, G. A. Carini, G. S. Camarda, R. B. James, “Characterization of Low Defect Cd<sub>0.9</sub>Zn<sub>0.1</sub>Te and CdTe Crystals for High Performance Frisch Collar Detectors,” IEEE Nuclear Science Symposium, San Diego, CA, Oct. 29-Nov. 3, 2006.
  4. A.E. Bolotnikov, G.S. Camarda, G.A. Carini, M. Fiederle, D.S. McGregor, W. McNeil, G.W. Wright, and R. B. James, “Performance Characteristics of Frisch-Grid CdZnTe Detectors,” IEEE Nuclear Science Symposium, Rome, Italy, Oct. 18-22, 2004.

- Patents:**
1. D.S. McGregor and R.A. Rojeski, "High Resolution Ionization Detectors and Array of Such Detectors," US-6,175,120; allowed January 16, 2001.
  2. D.S. McGregor, "Collimated Radiation Detector Assembly, Array of Collimated Radiation Detectors and Collimated Radiation Detector Module," US-6,781,132; allowed August 24, 2004.

*Note: Although the patents are affiliated with the invention described, they were filed before any DOE support was realized.*

#### Milestone Status Table:

<b>Complete</b>	<b>6/1/03</b> – Order CdZnTe material for the first year.
<b>Complete</b>	<b>7/1/03</b> – Design and begin fabrication of the collimator tubes.
<b>Complete</b>	<b>8/1/03</b> – Receive CdZnTe material. Begin fabrication of the detectors.
<b>Complete</b>	<b>9/1/03</b> – Complete first pocket-collimator devices. Begin resolution and directional sensitivity tests. Upgrade design.
<b>Complete</b>	<b>12/15/03</b> – Begin new pocket collimator design. Use both individual and corrugated approaches.
<b>Complete</b>	<b>2/15/04</b> – Complete the new sets of collimator/detector combinations. Begin tests for energy resolution and spatial resolution.
<b>Complete</b>	<b>4/15/04</b> – Assess preliminary results. Upgrade electronic readout if necessary.
<b>Complete</b>	<b>5/15/04</b> – Prepare report for progress on second year device fabrication and performance.
<b>Complete</b>	<b>5/31/04</b> – Complete testing of first year devices. Turn in report.
<b>Complete</b>	<b>6/1/04</b> – Order CdZnTe material for the second year.

<b>Complete</b>	<b>7/1/04</b> – Continue to manufacture detector/collimator elements and assemble the gamma ray camera. Order miniature electronics.
<b>Complete</b>	<b>8/1/04</b> – Receive CdZnTe material. Continue detector production and testing.
<b>Complete</b>	<b>1/1/05</b> – Complete assembly of the array. Test electronic readout and make appropriate changes. Begin tests with radiation sources and phantoms.
<b>Complete</b>	<b>3/15/05</b> – Assess preliminary results. Upgrade electronic readout if necessary.
<b>In progress</b>	<b>4/31/05</b> – Complete testing of the gamma ray camera and imaging array.
<b>In progress</b>	<b>5/15/05</b> – Prepare operating procedure and report on processes and equipment used for the array.
<b>Complete</b>	<b>5/31/05</b> – Turn in report
<b>Complete</b>	<b>6/1/05</b> – Order CdZnTe material for the third year. Design and build the required electronic readout system for the array.
<b>In progress</b>	<b>6/1/05</b> – Continue to manufacture detector/collimator elements and assemble the gamma ray camera. Order miniature electronics.
<b>Complete</b>	<b>7/1/05</b> – Receive CdZnTe material. Continue detector production and testing.
<b>Complete</b>	<b>11/1/05</b> – Complete assembly of the third array. Test electronic readout and make appropriate changes. Begin tests with radiation sources and phantoms.
<b>In progress</b>	<b>12/15/05</b> – Assess preliminary results. Upgrade electronic readout if necessary.
<b>In progress</b>	<b>4/31/06</b> – Complete testing of the gamma ray camera and imaging array.
<b>In progress</b>	<b>5/15/06</b> – Prepare operating procedure and report on processes and equipment used for the array.
<b>Complete</b>	<b>5/31/06</b> – Turn in final report

#### Budget Data:

	Dates	DOE Approved Total	Actual Spent
Year 1	7/2003 - 6/2004	\$116,265.00	\$81,486.00
Year 2	7/2004 – 6/2005	\$116,265.00	\$112,386.00
Year 3 (Total Project)	7/2003- 9/2005	\$349,921.00	\$156,049.00

The remaining balance of the project is \$0.00. The project supported two graduate students and three undergraduate students.

#### Detailed Description

## A. Introduction

CdZnTe has been studied for many years as a material for room-temperature, high energy resolution gamma ray detectors. Commercial and prototypical detectors are now available for medical imaging, industrial tomography and astrophysics. However, a simple device for accurately identifying radionuclides has not been available until recently with the advent of the semiconductor Frisch collar spectrometer [1-3]. Previous “single carrier” CdZnTe devices either lacked sufficient energy resolution, were complex to operate, or expensive to manufacture.

Energy resolution of planar CdZnTe devices is degraded by poor charge-carrier collection. The problem arises from electron and hole trapping, in which the hole trapping is much more deleterious than the electron trapping. Hole transport properties, such as mobility ( $\mu$ ) and lifetime ( $\tau$ ), within CdZnTe are generally poor compared to many other semiconductor materials. Various methods have been presented to improve the energy resolution of CdZnTe devices, with most methods concentrating on reducing the degrading effects of hole trapping, including variations using the small pixel effect [4], co-planar grids [5], and geometric weighting [6,7].

An ideal hand-held device for gamma ray spectroscopy and imaging applications is required to (1) operate at room temperature, (2) maintain low leakage current at high voltage bias, (3) provide high gamma ray energy resolution and (4) provide adequate gamma ray absorption efficiency. CdZnTe has shown promising results as a high energy resolution gamma ray detection material when coupled with a Frisch collar [1-3]. The device leakage current is low, mostly due to the relatively wide band gap, which also allows for room-temperature operation. Since CdZnTe is composed of high atomic number elements, it provides acceptable gamma ray absorption efficiency. Therefore, CdZnTe meets all aforementioned properties needed for a successful hand-held gamma ray spectrometer, as well as a gamma ray imaging array.

Yet, crystal imperfections in commercial CdZnTe material cause problems with severe hole trapping, which works to degrade the energy resolution and performance of the detectors. Single-carrier sensing, or single polarity, semiconductor detectors, using a similar concept as the Frisch grid ion chamber [10], have been investigated as a method to improve spectral performance of CdZnTe detectors by negating the deleterious effects of hole



trapping [3-9,11-14]. A relatively new and simple single carrier design, which is comprised of a CdZnTe planar detector wrapped in Teflon and copper tape, shows promising results as a room temperature operated high-resolution gamma ray spectrometer [1-3]. The copper tape serves as a virtual Frisch grid, while the Teflon tape serves as a resistive barrier to leakage current. The unique construction of the device, which is referred to as a “Frisch ring” or “Frisch collar” detector, is particularly suited for assembling into collimated arrays for imaging applications [2], in which the Frisch collar device is inserted into an extended collimator shielding tube. A set of such devices can be assembled into array modules. In the following work, the directional sensitivity performance of a Frisch collar CdZnTe planar detector is investigated for two different collimator lengths. Further, a simple model is developed to predict the relative change in detector count rate as a function of irradiation angle.

## B. Detector fabrication

Bulk CdZnTe material acquired from eV Products and Redlen Tech. , labeled as “counter grade”, were used to fabricate several Frisch ring detectors. The material was initially inspected with infrared (IR) microscope to locate a region containing relatively few visible defects. A diamond wire saw was then utilized to section volumes of low defect density from the bulk samples.

The extracted pieces were next shaped through grinding and lapping into right parallelepipeds. The sliced material was first ground using an L-shaped stainless steel jig to form the piece into a rectangular bar shape. Silicon carbide (SiC) papers of 2400 and 4000 grit were used in the grinding step, which were continuously cleaned by running water.

The ends of the bar-shaped crystals were hand lapped with alumina powders suspended in deionized (DI) water, starting with 3  $\mu\text{m}$  powders, and after a progression of diminishing sized powders, ending with 0.05  $\mu\text{m}$  powder on BUEHLER Chemomet polishing cloths. The 1 $\mu\text{m}$  and 0.3  $\mu\text{m}$  alumina powder solutions were used as intermediate polishing steps. At least 1  $\mu\text{m}$  of material was polished away from each of the sides. Mechanical polishing causes surface damage extending into the crystal bulk typically three times the size of the powder being used. Hence, while performing mechanical polishing, it is important to remove all of the surface damage caused in the previous step. Afterward, the

samples were rinsed with DI water and isopropyl alcohol before chemical treatment. The rinse was followed by a chemical etching step with a 2% bromine/methanol solution for 2-minute duration. The samples were then rinsed once more with isopropanol.

Gold was deposited on the ends of the crystal to form the ohmic contacts through an electroless deposition technique using gold chloride ( $\text{AuCl}_3$ ). The  $\text{AuCl}_3$  solution was deposited for eight minutes on each contact. When gold chloride is applied to the CdZnTe surface, a chemical reaction occurs, in which cadmium is removed from the surface and replaced by gold.

Surface passivation was performed as the final treatment to some of the devices. An ammonium fluoride ( $\text{NH}_4\text{F}$ )/DI water/hydrogen peroxide ( $\text{H}_2\text{O}_2$ ) solution of 2.68 g/17 ml/8ml was applied to the crystal surfaces for 10 minutes. Passivation provides an oxide layer that replaces tellurium rich surfaces left behind by the bromine/methanol etching step. This resistive oxide reduces side-surface leakage current substantially.

Finally, the passivated crystal was wrapped with thin Teflon tape, which acted as an insulating boundary. The Teflon was extended beyond the anode about 2 mm in order to avoid discharge between the collar and the anode. A thin copper shim was cut to size and used as the Frisch collar. The Frisch collar extended the entire length of the device, and was connected to the device cathode. In this manner, the Frisch collar was held at the cathode potential (or ground).

## C. Results

The results of this report is presented in three sessions as the spectroscopy results, angular dependency results of collimated device and charge collection characterization results. The details of the experimental setup for each study have been reported elsewhere [15-17]; however, the schematic setup of each study are presented in figures 1 through 3.

### ***C2. Spectroscopy results***

Pulse height spectra were collected from gamma rays sources of  $^{241}\text{Am}$ ,  $^{57}\text{Co}$ ,  $^{133}\text{Ba}$ ,  $^{198}\text{Au}$ ,  $^{137}\text{Cs}$  and  $^{235}\text{U}$ . The  $^{241}\text{Am}$ ,  $^{57}\text{Co}$ ,  $^{133}\text{Ba}$  and  $^{137}\text{Cs}$  samples were standard commercially available calibration sources. The  $^{198}\text{Au}$  was prepared through an  $(n,\gamma)$  reaction by irradiating a 13 mg sample of gold foil in the Kansas State University TRIGA Mk II nuclear reactor core

for 5 minutes at a fast neutron flux of  $3.5 \times 10^{12} \text{ cm}^{-2} \text{ s}^{-1}$  and thermal flux of  $4.3 \times 10^{12} \text{ cm}^{-2} \text{ s}^{-1}$ . The  $^{235}\text{U}$  source was in the form of a 93% enriched  $^{235}\text{U}$ -nitride solution. The electronic settings were consistent as previously explained for all measurements and energy resolutions reported for gamma ray photopeaks are without any electronic corrections.

An energy resolution of 9.10 % (5.41 keV) FWHM for the 59.5 keV spectral line of  $^{241}\text{Am}$  was obtained. The evaluated energy resolution is shown on Fig. 4 and does not take into consideration any contributions from electronic noise. The low noise floor and the high resolution of the device allows for the discernment of Cd and Te X-ray escape peaks, as labeled near 35 keV.

A  $^{57}\text{Co}$  spectrum is shown in Fig. 5. The energy resolution at the 122 keV photopeak is 4.91% (5.99 keV) FWHM and the 136 keV photopeak is clearly observed as a small peak on the right side of the 122 keV photopeak. The Cd and Te X-ray escape peaks are also visible. An electronic pulser peak is shown in the spectrum for noise comparisons, and is located near 191 keV on the energy scale.

Figs. 6 through 8 display the energy spectra for  $^{133}\text{Ba}$ ,  $^{198}\text{Au}$ , and  $^{137}\text{Cs}$ , respectively. An energy resolution of 7.55 % (6.04 keV) FWHM was achieved for the 80 keV photopeak of  $^{133}\text{Ba}$  as shown in Fig. 6a. The 356 keV photopeak of  $^{133}\text{Ba}$  exhibited an energy resolution of 2.33% (8.29 keV) FWHM (see Fig. 6b). The full energy peaks corresponding to the 276 keV, 302 keV and 382 keV emission energies of  $^{133}\text{Ba}$  are also clearly present in Fig. 6b. The 20 keV low noise cut off makes the device capable of detecting the cesium (Cs) X-rays seen in Fig. 6a. The  $^{198}\text{Au}$  spectrum is illustrated in Fig. 7. The 412 keV full energy peak resolution is 2.26% (9.31 keV) FWHM. Again, the Cd and Te X-ray escapes are observable. The 662 keV photopeak of  $^{137}\text{Cs}$  is observed with 1.45% (9.6 keV) FWHM energy resolution. The Compton continuum and backscatter peak are clearly seen in Fig. 8. Due to low noise, barium X-rays are also easily identified.

Fig. 9 shows the energy spectrum of  $^{235}\text{U}$  obtained from a low-activity 93% enriched  $^{235}\text{U}$ -nitride solution. The distance between the detector and the source was approximately 5 cm and the exposure time was 20 hours. All expected energy emissions, along with their branching ratios, are illustrated in Fig. 9. The clearly distinguishable spectral lines of  $^{235}\text{U}$  (Fig. 9) confirms that the insulated Frisch collar design incorporating bar-shaped CdZnTe material is fully capable of radioactive material identification.

The spectra presented in Figs 4 through 9 are all from one CdZnTe Frisch collar device, fabricated from counter grade materials acquired from eV Products. Some more recent results of similar CdZnTe Frisch collar device from Redlen Tech materials are presented in Figs 10 and 11.

## ***C2. Angular dependency results of collimated device***

The total number of counts collected for a certain source-detector angle can be evaluated by finding the net counts within the full energy peak of the pulse height spectrum (minus background). A complete set of source-detector angles with the evaluated net photopeak counts are presented Fig. 12 for the 4 cm and 8 cm collimators to compare the directional sensitivity of the two collimators. As expected, the longer collimator is more sensitive to changes in the source-detector angle. Between the source-detector angles of  $\pm 1^\circ$ , the detected counts from both collimators are nearly the same. However, once the gamma ray source was moved past the respective critical angle of each collimator, the shielding began to reduce the counts significantly. The second critical angle  $\alpha_{c2}$  for each collimator was experimentally observed to be at  $\pm 3^\circ$  and  $\pm 7^\circ$  for the 4 cm and 8 cm collimators, respectively.

The normalized counts from the experiment were compared to the analytical solutions, predicted. The comparisons between theory and experiment are shown in Figs. 13 and 14 for the 4 cm and 8 cm collimators, respectively. It can be understood from the figures that the two dimensional simple model is relatively acceptable in predicting the directional sensitivity of each collimator. Based on the model, the second critical angle occurs at  $\pm 6.6^\circ$  and  $\pm 2.9^\circ$  for the 4 cm and 8 cm collimators, respectively. By comparison, the values of  $\alpha_{c2}$  were experimentally verified as being  $\pm 7^\circ$  for the 4 cm collimator and  $\pm 3^\circ$  for the 8 cm collimator (see Figs. 12-14 ). The slight disagreement between theoretical and experimental data in Figs. 13 and 14 can be explained by a few factors. The predicted small plateau in counts in the analytical model for region 1 was not experimentally observed, in which it was assumed that the exposure angle and the efficiency of the CdZnTe detector accounted for the observed counts, and the effects of the copper, plastic, and Teflon tape were not included, thereby explaining, at least in part, the slight discrepancy. Subsequently, while considering the shielding effect of the tungsten collimator, the edge thicknesses (0.5 and 1.0 mm) for the

collimators were not taken into consideration. Overall, the simple analytical model predicts the performance of the collimated CdZnTe Frisch collar device quite well.

## ***C2. Charge collection characterization results***

The first configuration tested was the planar case. The collected spectra are shown in Fig. 15. Note the nearly linear decrease in the amount of charge collected in the photopeaks. The full length Frisch collar spectra exhibited the greatest change in spectra from the planar case. A plot of the collected full length Frisch collar spectra is given in Fig. 16.

Using the location of the full energy photoelectric peak in each of the spectra in Figs. 15 and 16, the corresponding CCE of each spectrum was calculated. These data points were then plotted alongside the theoretically predicted CCE profiles of each device configuration in Fig. 17. A reasonable match between theory and measurement was found for both cases. As noted previously, several other Frisch collars of varying lengths were also tested. The resulting CCE profiles are shown in Fig. 18.

## **D. Array of detectors**

Developing the imaging array of CdZnTe Frisch collar detectors is still under investigation at SMART lab, KSU. One of the earliest designs for a 2x2 module (four W-collimated CdZnTe Frisch collar detectors) is shown in Figs. 19. The detectors were placed inside the 8.0 cm long tungsten collimators. Every single device was tested before and after mounting inside the W-collimators, individually, using  $^{241}\text{Am}$  gamma ray source. The results of the spectral test were similar to what presented in Fig. 4. A 4-channel preamplifier (Fig. 19-b) was employed to read the 2x2 module in order to take the image; however, since the 4-channel preamplifier was not specifically designed for the CdZnTe devices capacitance, no image was successfully taken with the assembled 2x2 module of CdZnTe detector.

Recently, due to fabricating more spectroscopic grade CdZnTe Frisch collar detectors, more devices were available for the imaging array. Fig. 20 shows the CdZnTe Frisch collar detectors wired with TIN copper and soldered to a PC board which is connected to the BNC connector aluminum board. A study to determine the appropriate electronic read out and MCA card for a 16-channel array of CdZnTe detectors is still under investigation through ORTEC and some other electronic manufacturers. No electronic package has been

provided to read and acquire the images from the module of 4x4 and 3x3 W-collimated CdZnTe Frisch collar detectors presented in Fig. 21.

#### E. References

- [1] D. S. McGregor and R. A. Rojeski, US Patent No. 6,175,120, January 16, 2001.
- [2] D.S. McGregor, US Patent No. 6,781,132, August 24, 2004.
- [3] W.J. McNeil, D.S. McGregor, A.E. Bolotnikov, G.W. Wright, and R.B. James, Appl. Phys. Lett., **84** (2004) 1988.
- [4] H.H. Barrett, J.D. Eskin, H.B. Barber, Phys. Rev. Lett. **75** (1995) 156.
- [5] P.N. Luke, IEEE Trans. Nucl. Sci., **NS-42** (1995) 207.
- [6] H.I. Malm, C. Canali, J.W. Mayer, M.A. Nicolet, K.R. Zanio, W. Akutagawa, Appl. Phys. Lett., **26** (1975) 344.
- [7] D. S. McGregor, and R. A. Rojeski, IEEE Trans. on Nucl. Sci., **46** no. 3 (1999) 250.
- [8] D. S. McGregor, Z. He, H. A. Seifert, R. A. Rojeski, and D. K. Wehe, IEEE Trans. Nucl. Sci., **45** (1998) 443.
- [9] A.E. Bolotnikov, G. S. Camarda, G. A. Carini, G. W. Wright, R. B. James, D. S. McGregor, and W. McNeil, Proc. SPIE, **5540** (2004) 33.
- [10] O. Frisch, British Atomic Energy Report, BR-49 (1944).
- [11] K. Parnham, J. B. Glick, Cs. Szeles, K. G. Lynn, J. Crys. Growth, **214/215** (2000) 1152.
- [12] G. Montemont, M. Arques, L. Verger, and J. Rustique, IEEE Trans. Nucl. Sci., **48** (2001) 278.
- [13] L.Cirignano, H.Kim, K.Shah, M.Klugerman, P.Wong, M.Squillante, and L.Li, Proceedings of the SPIE, **5198** (2004) 1.
- [14] A. E. Bolotnikov, G. S. Camarda, G. A. Carini, G. W. Wright, L. Li, A. Burger, M. Groza and R. B. James, Phys. Stat. sol. (c) **2** (2005) 1495.
- [15] A. Kargar, A.M. Jones, W.J. McNeil, M.J. Harrison, D.S. McGregor, Nucl. Instr. and Meth. A **558** (2006) 497
- [16] A. Kargar, A.M. Jones, W.J. McNeil, M.J. Harrison, D.S. McGregor, Nucl. Instr. and Meth. A **562** (2006) 262
- [17] M.J. Harrison, A. Kargar, D.S. McGregor, Nucl. Instr. and Meth, In press.

F. Figures

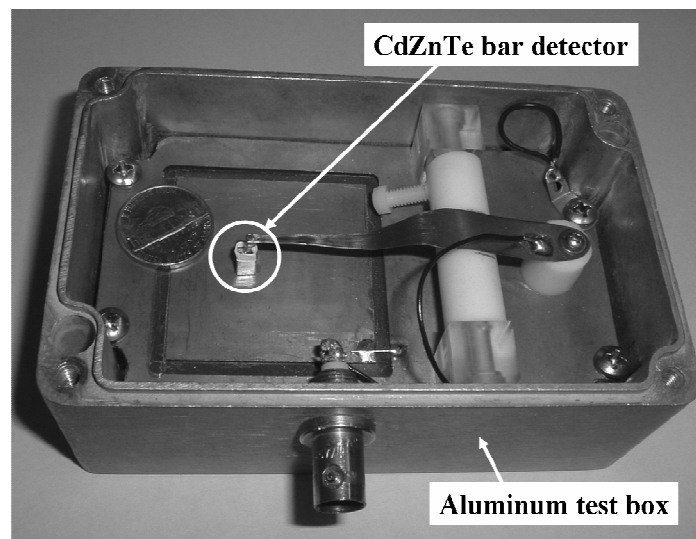


**Fig. 1.** The Experiment apparatus and the aluminum test box with an installed CdZnTe Frisch collar device.

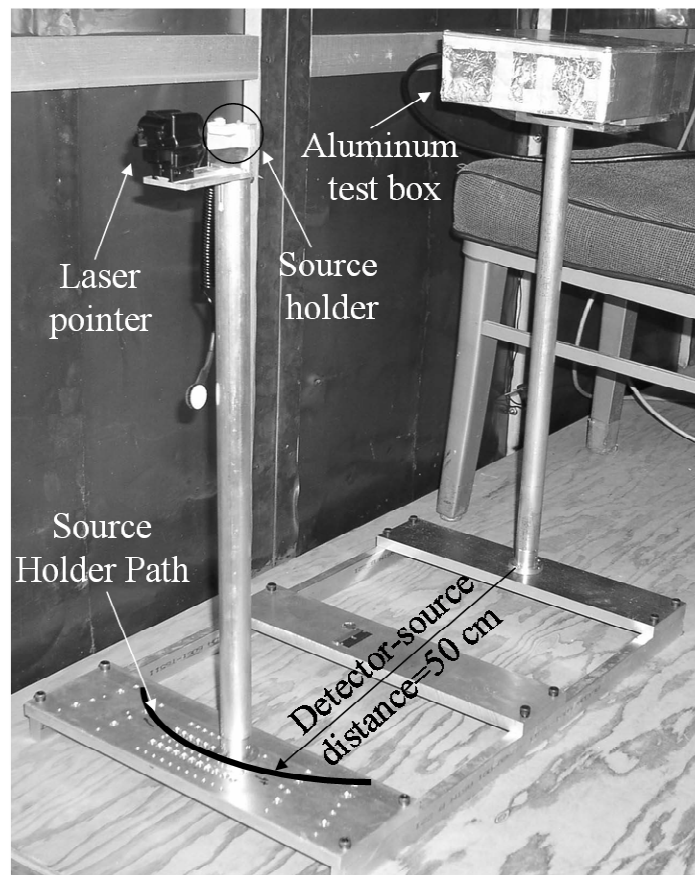


**Fig. 2a** The aluminum test stage inside the Faraday cage.

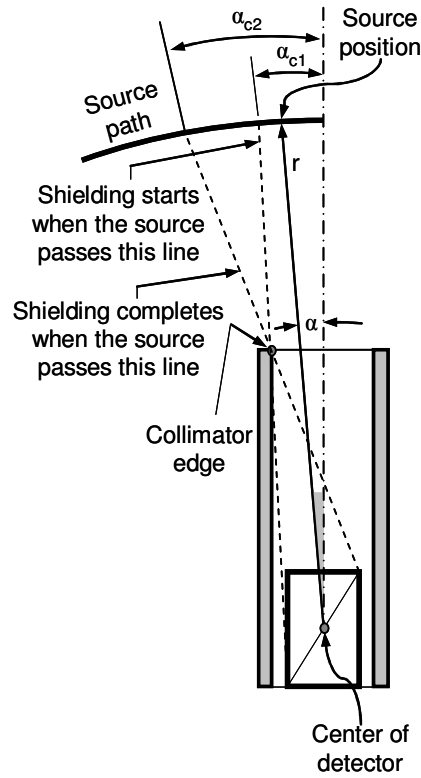


**Fig. 2b** The Schematic picture of the two-dimensional model for detector–collimator–source positions showing the two critical angles and the source position with respect to detector–collimator assembly ( $r=50$  cm).

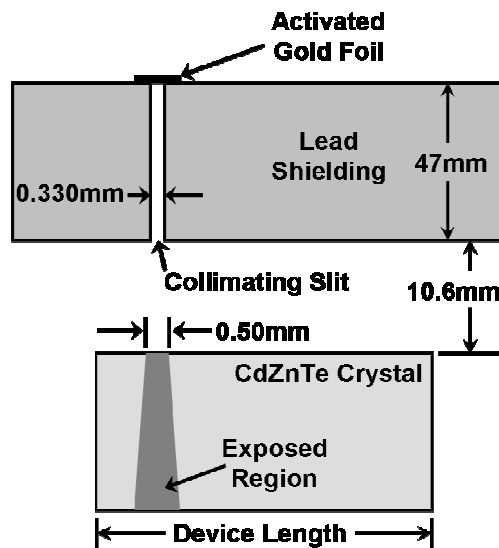


**Fig. 3** Arrangement of activated gold foil source and lead shielding with respect to the CdZnTe detector.



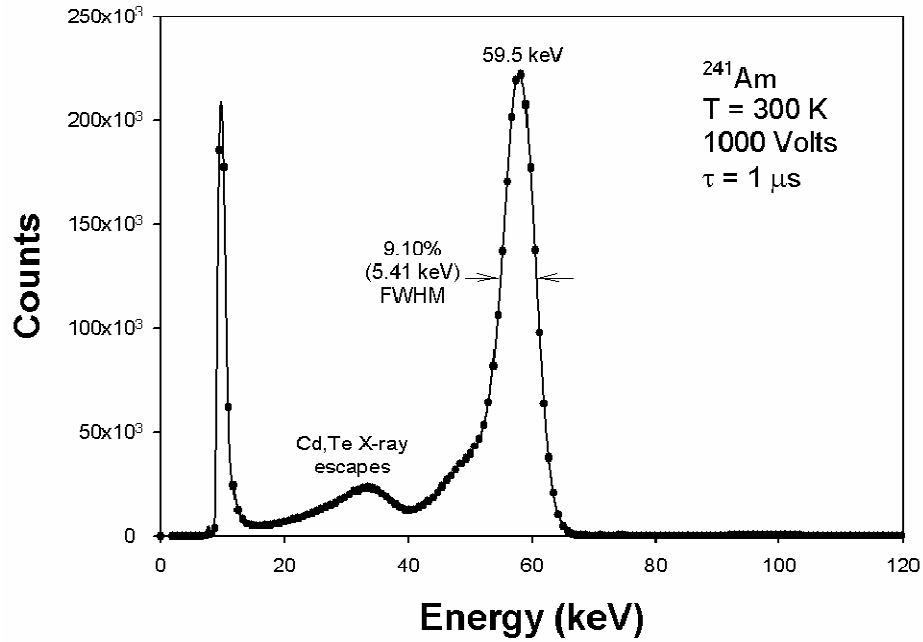


**Fig. 4** Room temperature spectra of a <sup>241</sup>Am source from the 3.4 mm x 3.4 mm x 5.7 mm CdZnTe semiconductor detector.

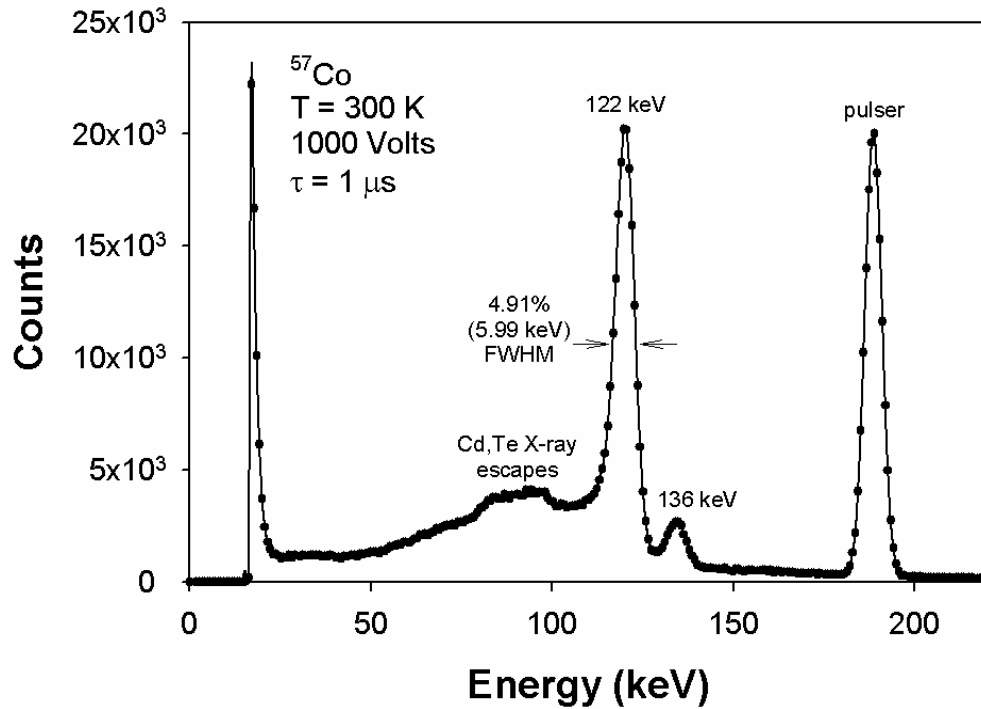
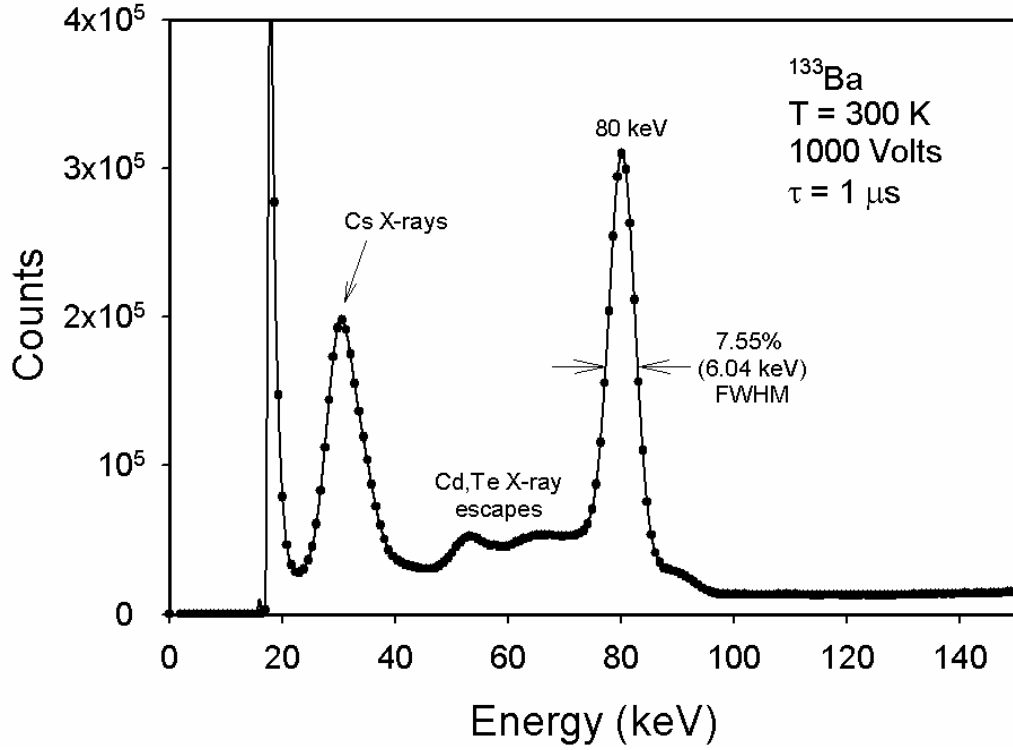
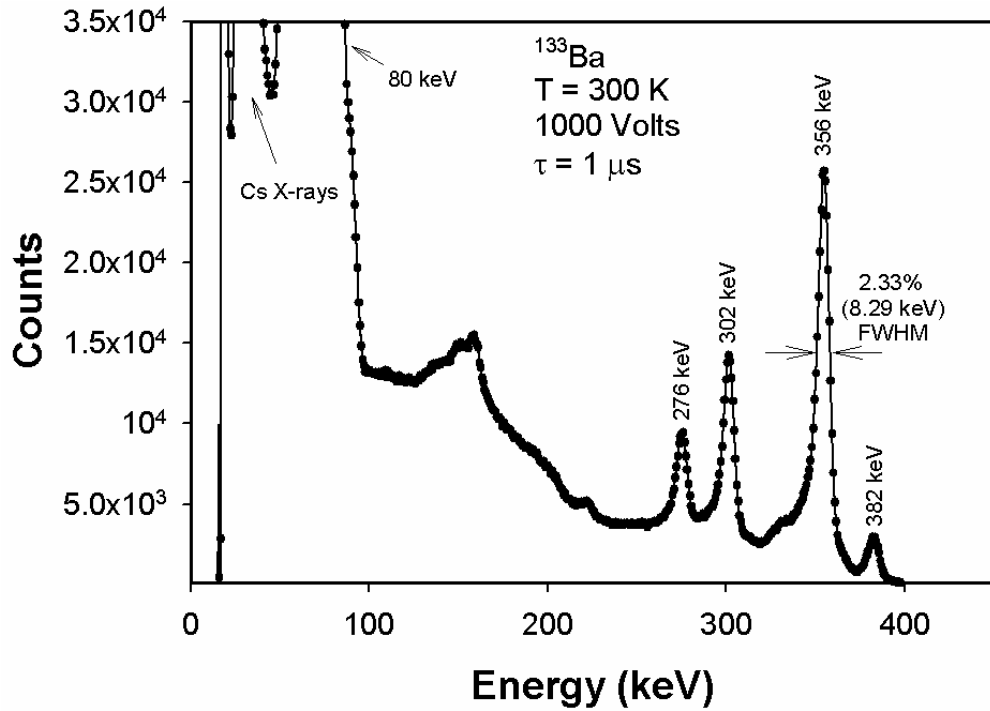


**Fig. 5** Room temperature spectra of a <sup>57</sup>Co source from the 3.4 mm x 3.4 mm x 5.7 mm CdZnTe semiconductor detector.



(a)



(b)

**Fig.s 6** Room temperature spectra of a  $^{133}\text{Ba}$  source from the 3.4 mm x 3.4 mm x 5.7 mm CdZnTe semiconductor detector (a) at low energies (b) at higher energies.

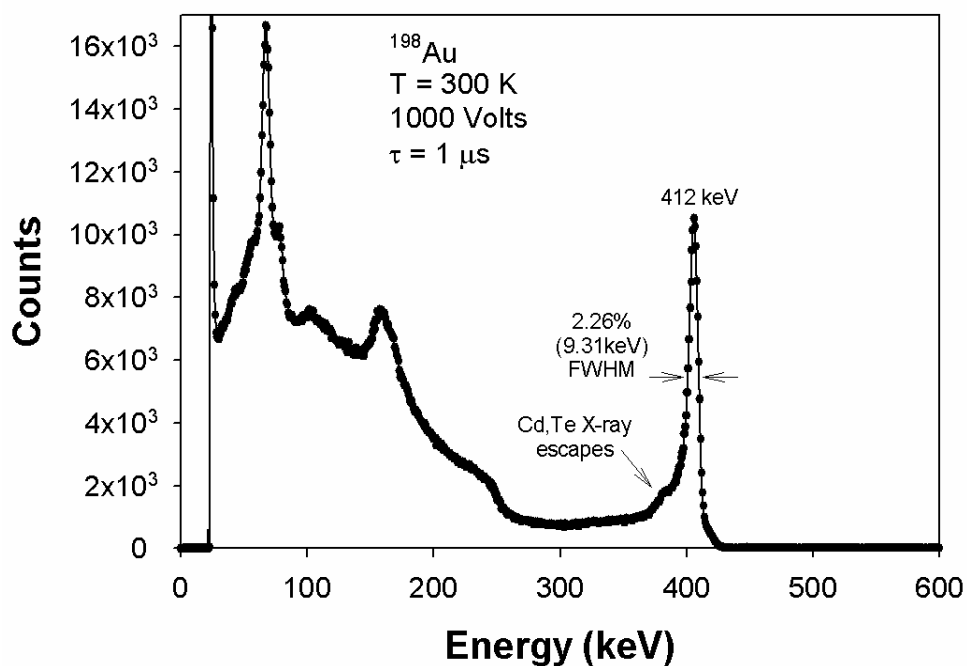


**Fig. 7** Room temperature spectra of a  $^{198}\text{Au}$  source from the 3.4 mm x 3.4 mm x 5.7 mm CdZnTe semiconductor detector.

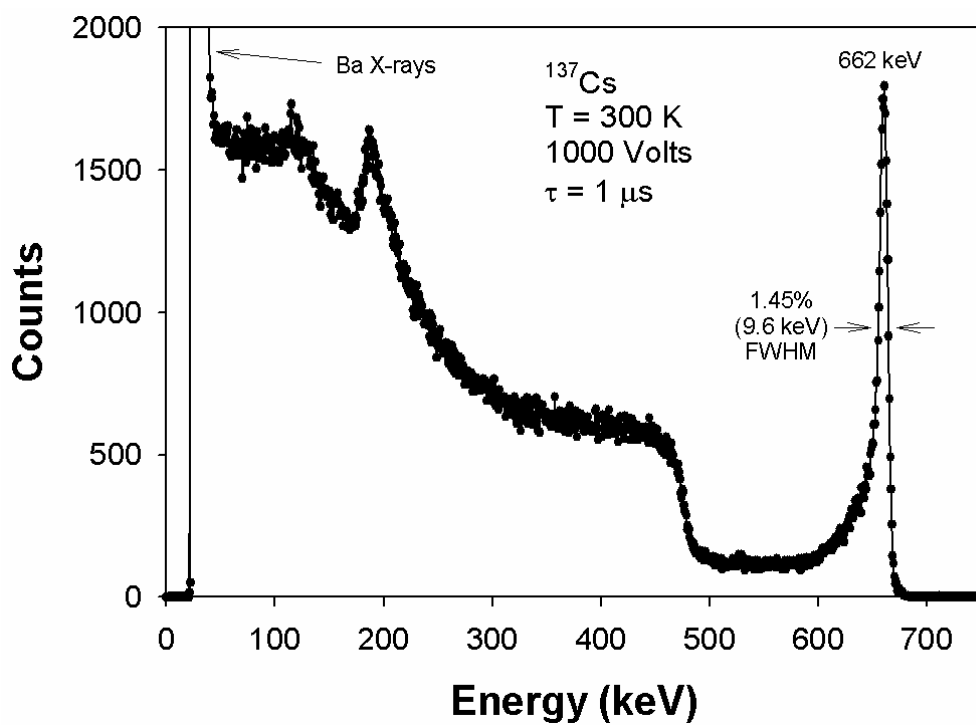


**Fig. 8** Room temperature spectra of a  $^{137}\text{Cs}$  source from the 3.4 mm x 3.4 mm x 5.7 mm CdZnTe semiconductor detector.

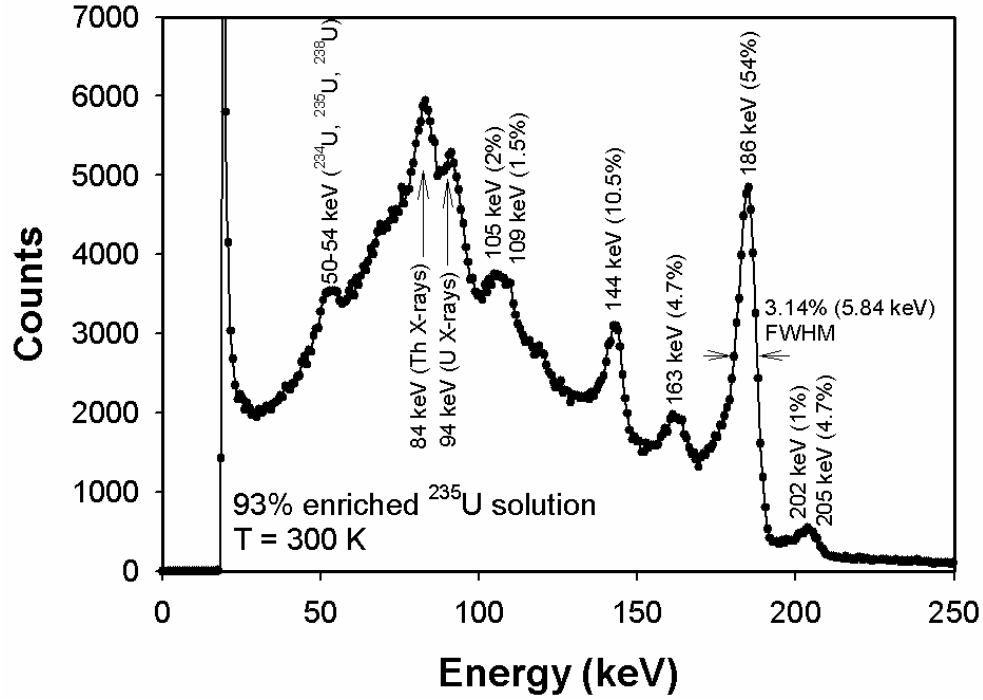


**Fig. 9** Room temperature spectra of a  $^{235}\text{U}$  source from the 3.4 mm x 3.4 mm x 5.7 mm CdZnTe semiconductor detector.

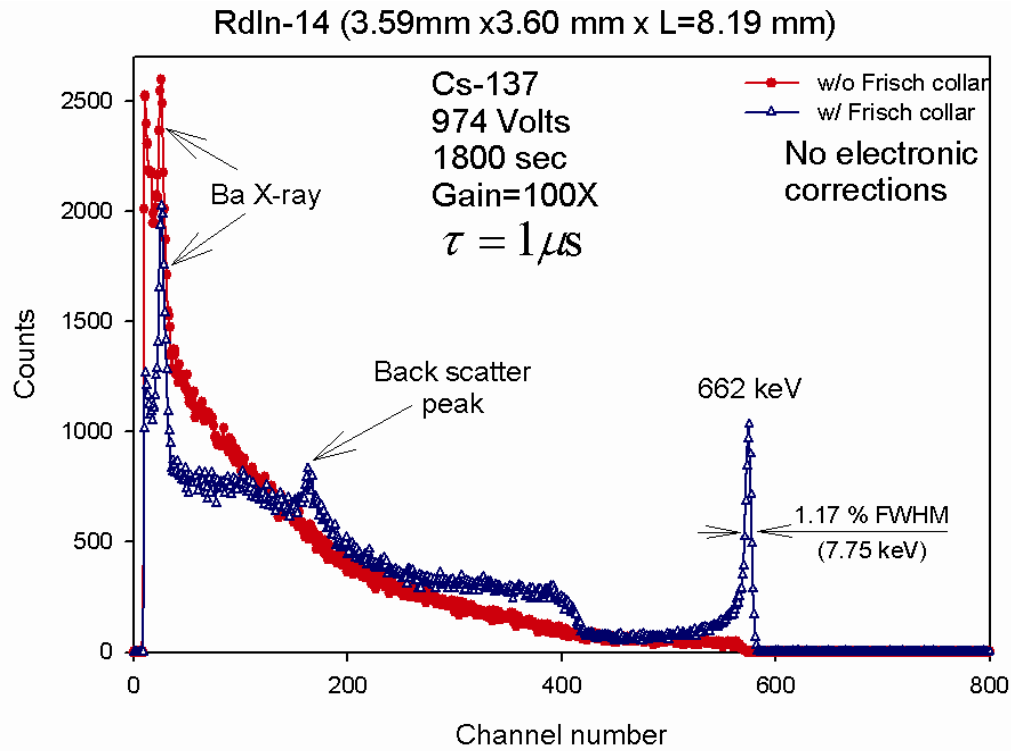


**Fig. 10** Room temperature spectra of a  $^{137}\text{Cs}$  source from the 3.59 mm x 3.60 mm x 8.19 mm CdZnTe semiconductor detector.

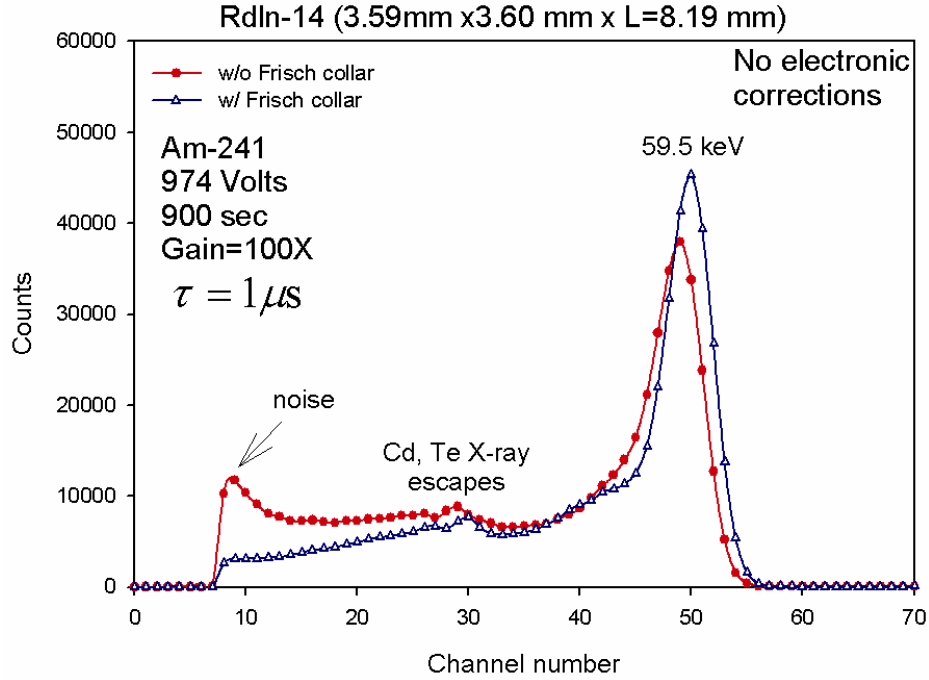


**Fig. 11** Room temperature spectra of a  $^{241}\text{Am}$  source from the 3.59 mm x 3.60 mm x 8.19 mm CdZnTe semiconductor detector.

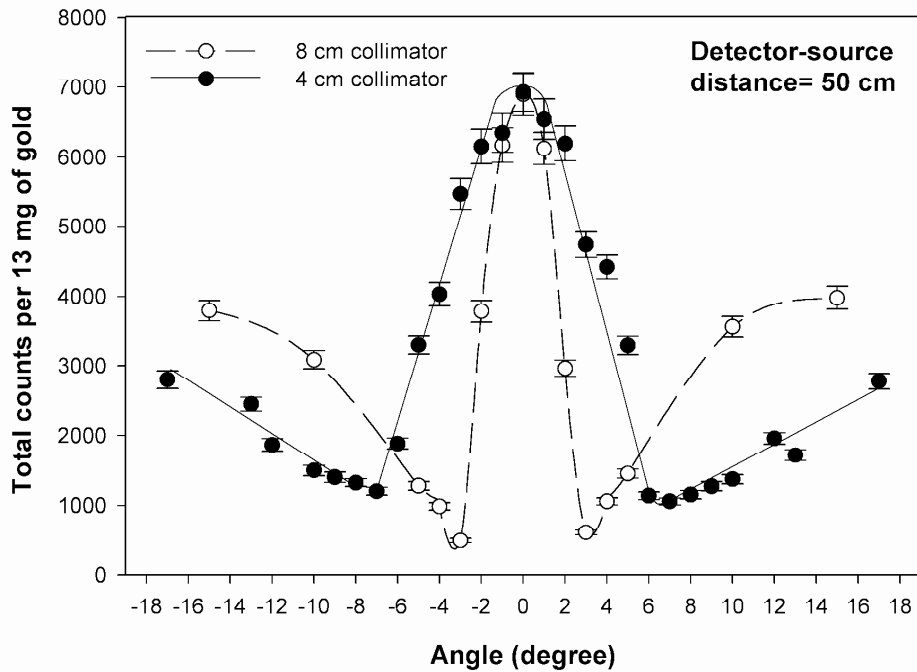


**Fig. 12** The experimental angular dependency of counts  $13 \pm 2 \text{ mg } ^{198}\text{Au}$  sources with the 3.4 mm x 3.4 mm x 5.8 mm CdZnTe semiconductor detector for the 4 cm and 8 cm long tungsten collimators.

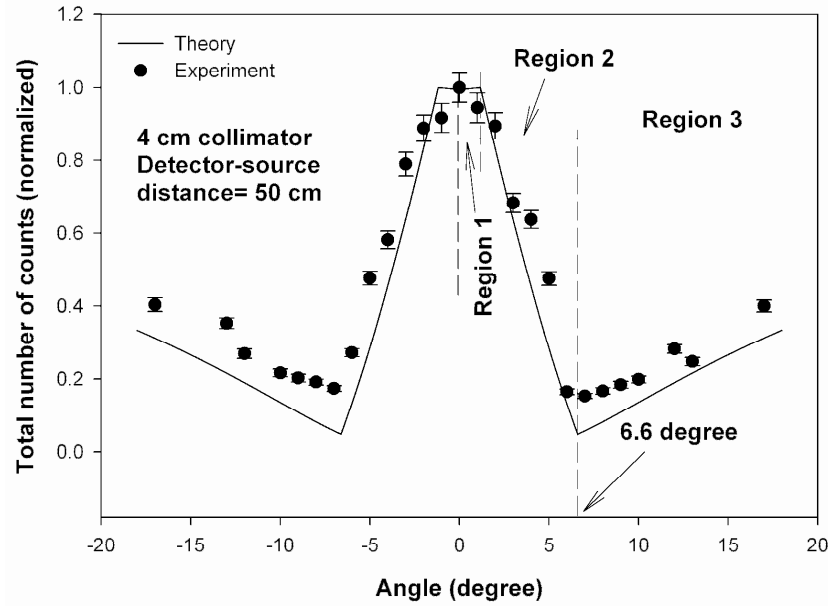


**Fig. 13** The experimental and theoretical angular dependency of counts for  $13 \pm 2$  mg  $^{198}\text{Au}$  sources with the 3.4 mm x 3.4 mm x 5.8 mm CdZnTe semiconductor detector inside the 4 cm long tungsten collimator.

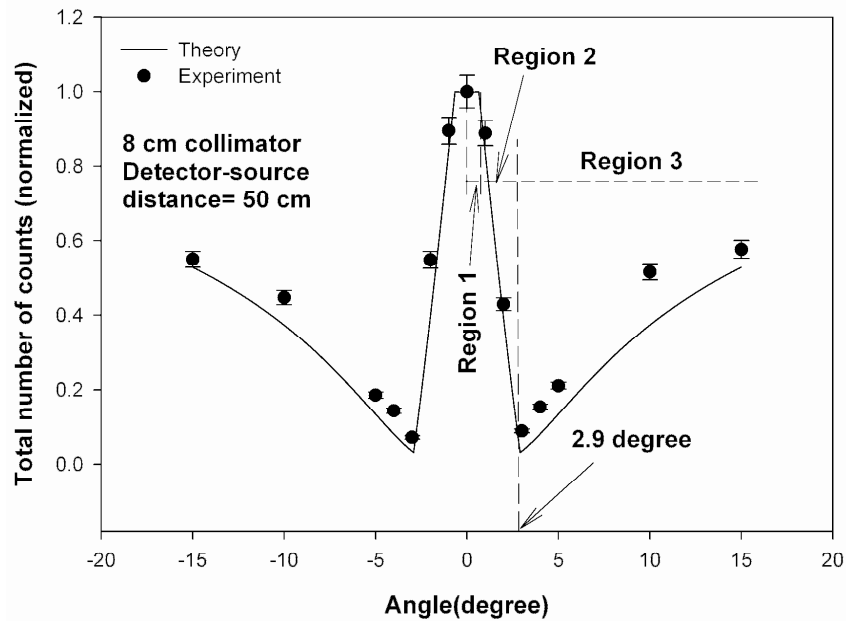


**Fig. 14** The experimental and theoretical angular dependency of counts for  $13 \pm 1$  mg  $^{198}\text{Au}$  sources with the 3.4 mm x 3.4 mm x 5.8 mm CdZnTe semiconductor detector inside the 8 cm long tungsten collimator.

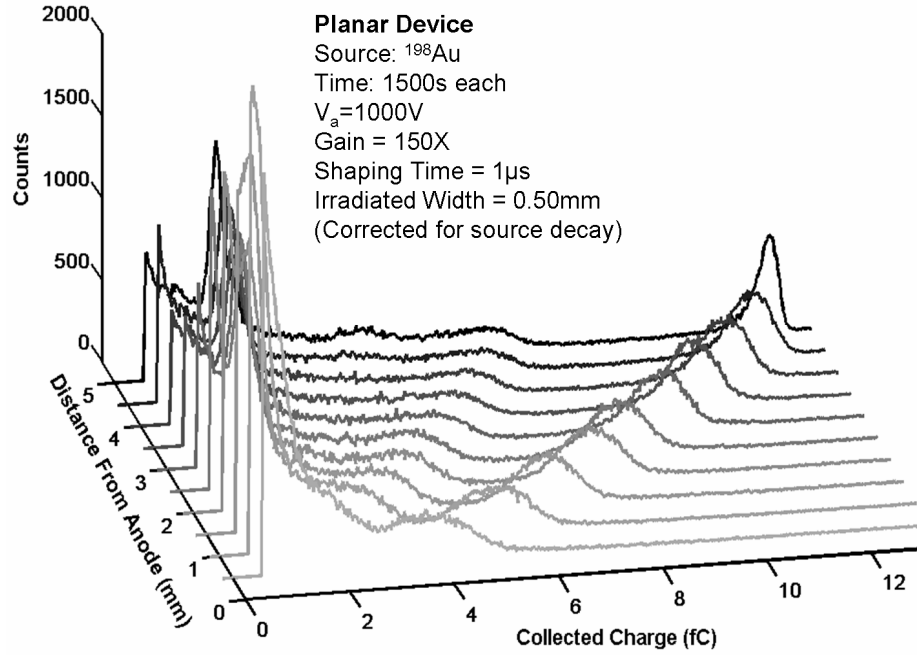


**Fig. 15** Pulse height spectra collected from the planar configuration of a  $3.4 \times 3.4 \times 5.5 \text{ mm}^3$  CdZnTe device. MCA channel numbers have been converted to an equivalent charge collected by using (2)-(4).

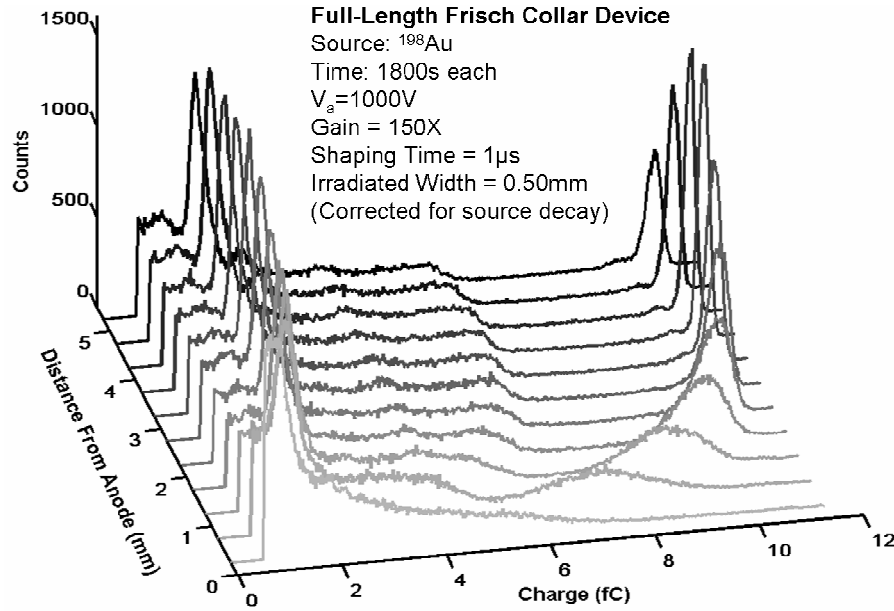


**Fig. 16** Pulse height spectra collected from the full length Frisch collar configuration of a  $3.4 \times 3.4 \times 5.5 \text{ mm}^3$  CdZnTe device. MCA channel numbers have been converted to an equivalent charge collected by using (2)-(4).

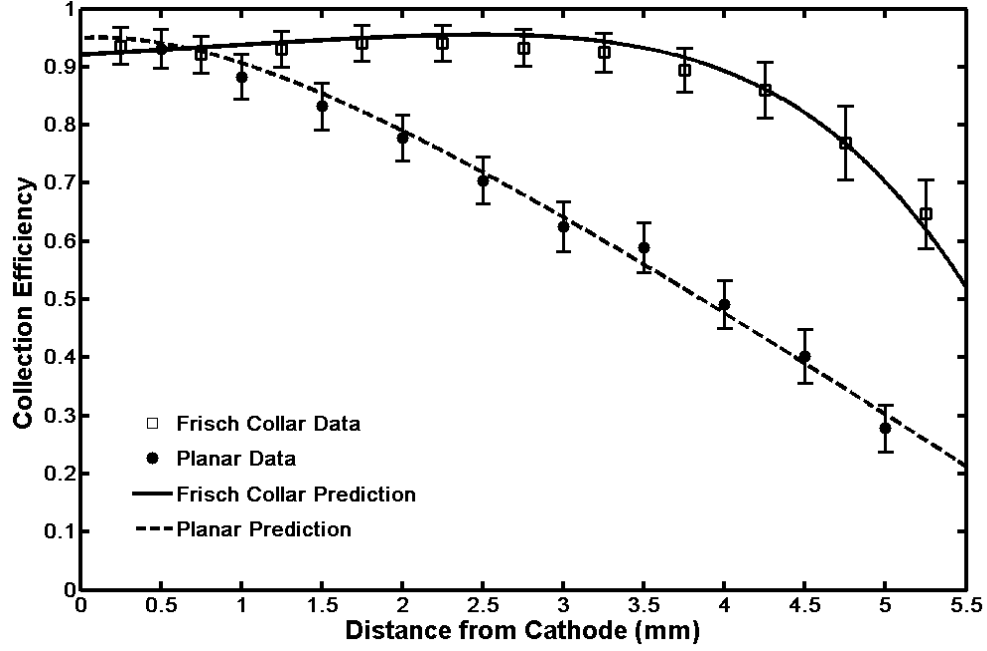


**Fig. 17.** Measured values and theoretically predicted curves of the CCE of a 3.4 x 3.4 x 5.5 mm<sup>3</sup> CdZnTe detector.

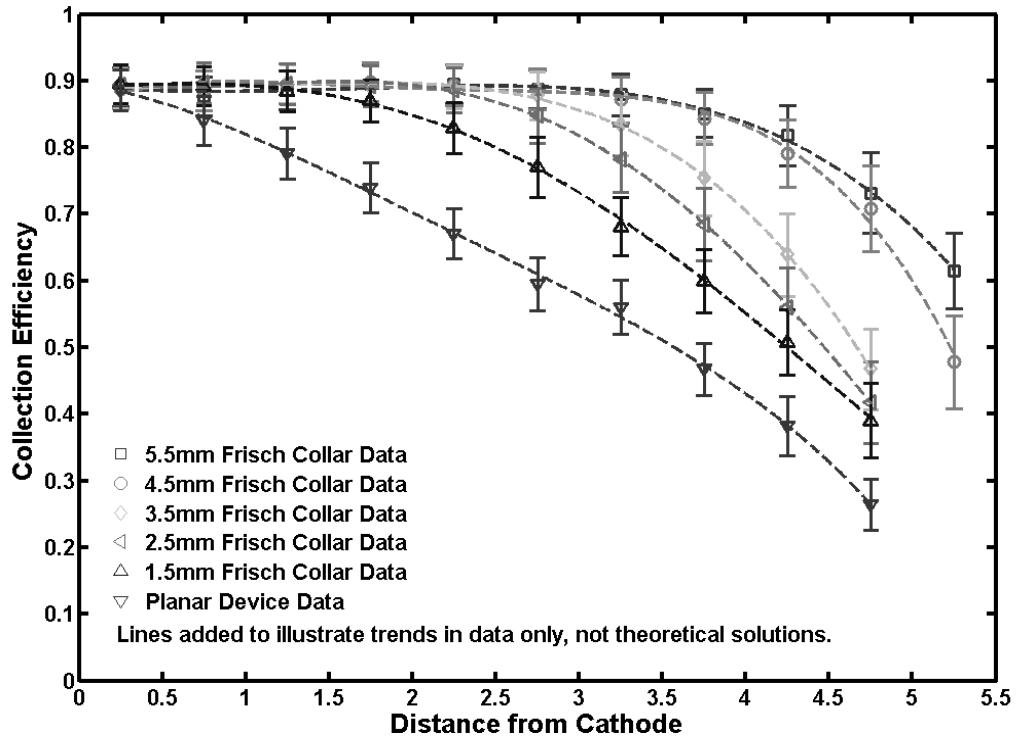
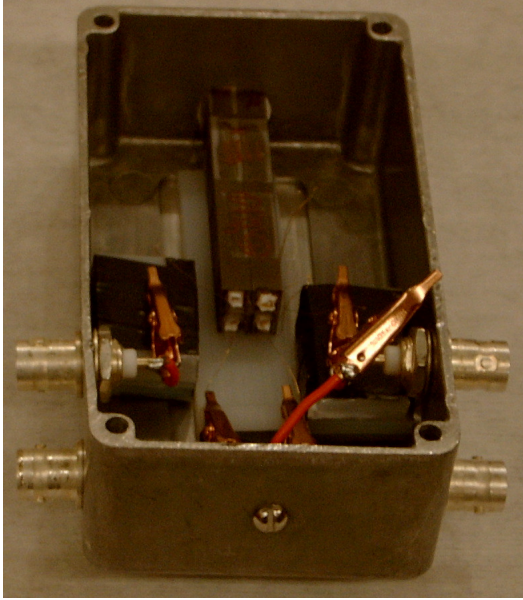
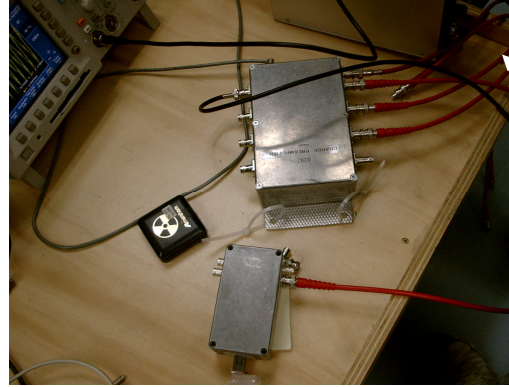


**Fig. 18** Measured CCE profiles of various length Frisch collar configurations of a 3.4 x 3.4 x 5.5 mm<sup>3</sup> CdZnTe detector



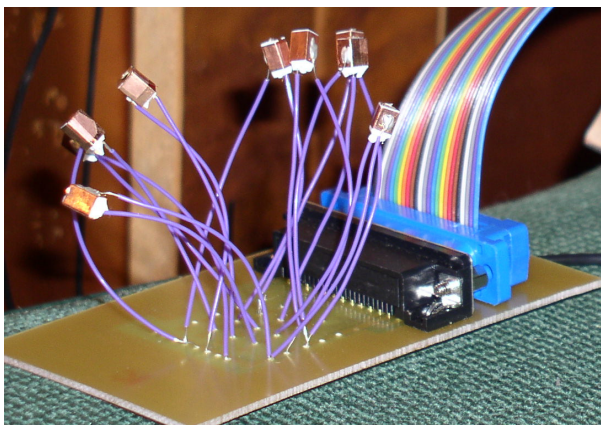


(a)

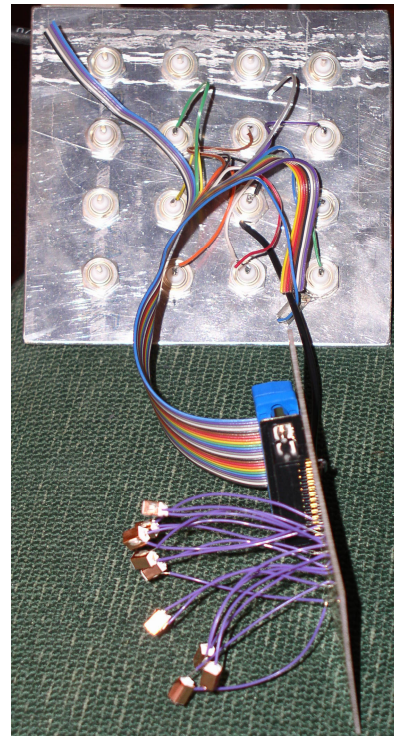


(b)

**Fig. 19.** The 2x2 module of four W-collimated CdZnTe Frisch collar detectors (a) the aluminum test box with W-collimated detectors (b) the testing stage with the 4-channel preamplifier.



(a)



(b)

**Fig. 20.** The preliminary works on assembling the detectors into imaging arrays (a) the detectors are wired with TIN copper to the board (b) the board is connected to BNC connector aluminum board.

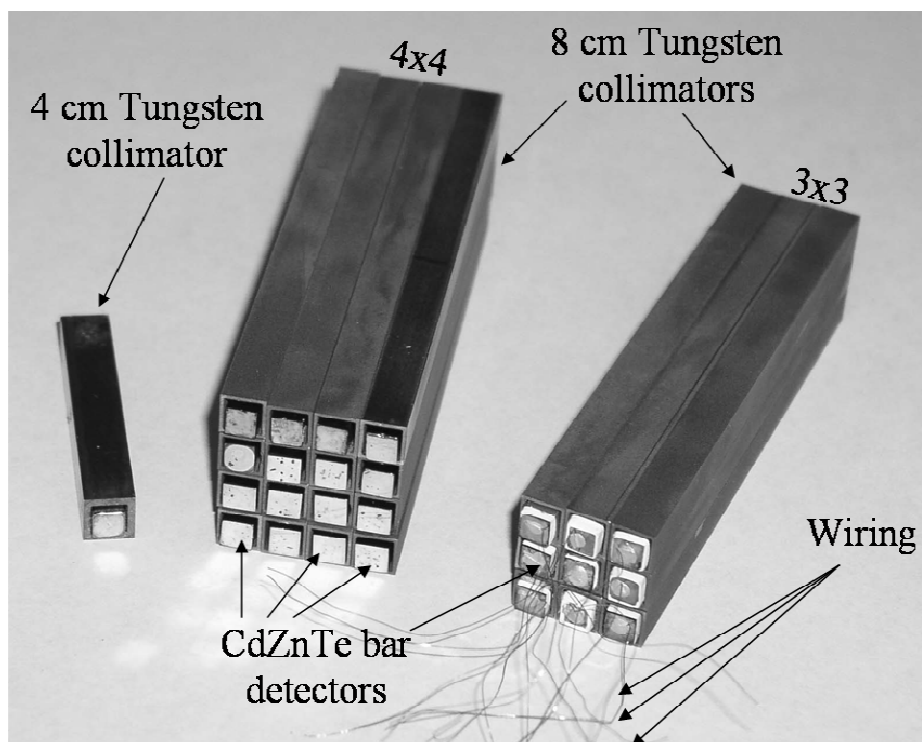


**Fig. 21** The module of 4x4 and 3x3 W-collimated CdZnTe Frisch collar detectors.